Title	An injectable elastin-based gene delivery platform for dose-dependent modulation of angiogenesis and inflammation for critical limb ischemia
Author(s)	Dash, Biraja C.; Thomas, Dilip; Monaghan, Michael; Carroll, Oliver; Chen, Xizhe; Woodhouse, Kimberly; O'Brien, Timothy; Pandit, Abhay
Publication Date	2015-10
Publication Information	Dash, BC,Thomas, D,Monaghan, M,Carroll, O,Chen, XZ,Woodhouse, K,O'Brien, T,Pandit, A (2015) 'An injectable elastin-based gene delivery platform for dose-dependent modulation of angiogenesis and inflammation for critical limb ischemia'. Biomaterials, 65 :126-139.
Publisher	Elsevier
Link to publisher's version	http://www.sciencedirect.com/science/article/pii/S0142961215005517
Item record	http://hdl.handle.net/10379/5625
DOI	http://dx.doi.org/10.1016/j.biomaterials.2015.06.037

Elsevier Editorial System(tm) for Biomaterials
Manuscript Draft

Manuscript Number: jbmt32689R1

Title: An Injectable Elastin-based Gene Delivery Platform for Dose-dependent Modulation of Angiogenesis and Inflammation for Critical Limb Ischemia

Article Type: FLA Original Research

Section/Category: Biomaterials and Regenerative Medicine (BRM)

Keywords: Elastin-like polypeptide; hollow spheres; critical limb ischemia; gene therapy; angiogenesis; inflammation

Corresponding Author: Prof. Abhay Pandit, PhD

Corresponding Author's Institution: National University of Ireland, Galway

First Author: Biraja Dash, PhD

Order of Authors: Biraja Dash, PhD; Dilip Thomas; Michael Monaghan, PhD; Oliver Carroll, PhD; Xizhe Chen, PhD; Kimberly Woodhouse, PhD; Timothy O'Brien, PhD; Abhay Pandit, PhD

Abstract: Critical limb ischemia is a major clinical problem. Despite rigorous treatment regimes, there has been only modest success in reducing the rate of amputations in affected patients. Reduced level of blood flow and enhanced inflammation are the two major pathophysiological changes that occur in the ischemic tissue. The objective of this study was to develop a controlled dual gene delivery system capable of delivering therapeutic plasmid eNOS and IL-10 in a temporal manner. In order to deliver multiple therapeutic genes, an elastin-like polypeptide (ELP) based injectable system was designed. The injectable system was comprised of hollow spheres and an in situ-forming gel scaffold of elastin-like polypeptide capable of carrying gene complexes, with an extended manner release profile. In addition, the ELP based injectable system was used to deliver human eNOS and IL-10 therapeutic genes in vivo. A subcutaneous dose response study showed enhanced blood vessel density in the treatment groups of eNOS (20 μg) and IL-10 (10 μg)/eNOS (20 μg) and reduced inflammation with IL-10 (10 μg) alone. Next, we carried out a hind-limb ischemia model comparing the efficacy of the following interventions; Saline; IL-10, eNOS and IL-10/eNOS. The selected dose of eNOS, exhibited enhanced angiogenesis. IL-10 treatment groups showed reduction in the level of inflammatory cells. Furthermore, we demonstrated that eNOS up-regulated major proangiogenic growth factors such as vascular endothelial growth factors, platelet derived growth factor B, and fibroblast growth factor 1, which may explain the mechanism of this approach. These factors help in formation of a stable vascular network. Thus, ELP injectable system mediating non-viral delivery of human IL10-eNOS is a promising therapy towards treating limb ischemia.

An Injectable Elastin-based Gene Delivery Platform for Dose-dependent Modulation of Angiogenesis and Inflammation for Critical Limb Ischemia

Biraja C. Dash[1], Dilip Thomas[2,5], Michael Monaghan[3], Oliver Carroll[2], Xizhe Chen[5] Kimberly Woodhouse[4], Timothy O'Brien[5] and Abhay Pandit[2]

1. Yale Cardiovascular Research Center, Section of Cardiovascular Medicine, Department of Internal Medicine, Yale School of Medicine, New Haven, CT 06510, USA.
2. Centre for Research in Medical Devices (CÚRAM), National University of Ireland, Galway, Ireland.
3. Department of Cell and Tissue Engineering, Fraunhofer Institute for Interfacial Engineering and Biotechnology (IGB), 70569 Stuttgart, Germany.
4. Department of Chemical Engineering, Queen's University, Kingston, ON, Canada.
5. Regenerative Medicine Institute, National Centre for Biomedical Engineering Science, National University of Ireland, Galway.

Address correspondence to: Prof. Abhay Pandit, Centre for Research in Medical Devices (CÚRAM), National University of Ireland, Galway, Ireland.
E-mail: abhay.pandit@nuigalway.ie.

Abstract

Critical limb ischemia is a major clinical problem. Despite rigorous treatment regimes, there has been only modest success in reducing the rate of amputations in affected patients. Reduced level of blood flow and enhanced inflammation are the two major pathophysiological changes that occur in the ischemic tissue. The objective of this study was to develop a controlled dual gene delivery system capable of delivering therapeutic plasmid eNOS and IL-10 in a temporal manner. In order to deliver multiple therapeutic genes, an elastin-like polypeptide (ELP) based injectable system was designed. The injectable system was comprised of hollow spheres and an *in situ*-forming gel scaffold of elastin-like polypeptide capable of carrying gene complexes, with an extended manner release profile. In addition, the ELP based injectable system was used to deliver human eNOS and IL-10 therapeutic genes *in vivo*. A subcutaneous dose response study showed enhanced blood vessel density in the treatment groups of eNOS (20 μg) and IL-10 (10 μg)/eNOS (20 μg) and reduced inflammation with IL-10 (10 μg) alone. Next, we carried out a hind-limb ischemia model comparing the efficacy of the following interventions; Saline; IL-10, eNOS and IL-10/eNOS. The selected dose of eNOS, exhibited enhanced angiogenesis. IL-10 treatment groups showed reduction in the level of inflammatory cells. Furthermore, we demonstrated that eNOS up-regulated major proangiogenic growth factors such as vascular endothelial growth factors, platelet derived growth factor B, and fibroblast growth factor 1, which may explain the mechanism of this approach. These factors help in formation of a stable vascular network. Thus, ELP injectable system mediating non-viral delivery of human IL10-eNOS is a promising therapy towards treating limb ischemia.

Keywords: Elastin-like polypeptide, hollow spheres, critical limb ischemia, gene therapy, angiogenesis, inflammation

Introduction

Critical limb ischemia (CLI) is a manifestation of peripheral artery disease (PAD), caused by the obstruction of blood flow to the limb [1, 2]. CLI affects around 500–1000 per million of the population in Europe and North America every year. Without endovascular treatment, CLI patients are at a very high risk of amputation, leading to significant morbidity and mortality. Thus, it is considered a critical public health issue worldwide. The fundamental goal of CLI treatment is to relieve ischemic rest pain, heal ulcers, prevent limb loss and improve the quality of life, thereby extending the survival of the patient [1]. Therefore exploring new and more effective strategies for revascularization of ischemic limbs is imperative. A viable therapeutic alternative is necessary to promote angiogenesis through the delivery of proangiogenic drug (genes and growth factors) and/or cell delivery for angiogenesis [3-5].

Understanding the pathophysiology of limb ischemia is a necessity for finding an effective treatment [4]. The two major pathways contributing to pathophysiology of this disease are inflammation and angiogenesis. During an ischemic insult, most tissues in the body attempt to compensate for low levels of blood supply by mechanisms of angiogenesis, arteriogenesis, vascular remodeling, and hematopoiesis [3]. Among many proangiogenic growth factors, vascular endothelial growth factor (VEGF), platelet-derived growth factor (PDGF), and fibroblast growth factors (FGF) play an important role in regulating angiogenesis in an ischemic tissue [6-9]. Ischemia also induces an inflammatory response, triggered by the breakdown products of the degenerating tissue. The major proinflammatory cytokines released during this time are IL-1β, TNFα, and IL-6 [10, 11]. Also, IL-10, an anti-inflammatory cytokine, has been shown to be up-regulated in the ischemic tissue [12]. Despite the endogenous up-regulation of the proangiogenic factors, this is insufficient to compensate for the progressive deterioration of

the tissue, due to the lack of blood supply. Hence, delivering soluble growth factors/cytokines or therapeutic genes could help in slowing down the tissue damage and promote tissue repair [7, 9, 13].

Non-viral gene therapy is an evolving field [14, 15]. Various cationic polymers have been developed so far to form a complexes of *p*DNA/polymer (polyplexes) to transfect the gene of interest to cells [16-18]. The polyplex helps in reduction of the size of the *p*DNA and helps it in crossing the cell membrane barrier efficiently. Also, *p*DNA micro-carriers have been developed to load and release genes of interest in a spatio-temporal manner. Recently, elastin-like polypeptide (ELP) has been used to fabricate hollow micro-spheres of a gene delivery depot [19]. ELP is used for various biomedical applications due to its biodegradable, non-toxic, non-inflammatory properties and efficient pharmacokinetics for the delivery of therapeutics [20, 21].

In this study, a combined gene therapy approach for angiogenesis and inflammation has been considered for the treatment of CLI. It was hypothesized that the dual release of eNOS and IL-10 using an ELP based delivery platform will modulate inflammation and increase the blood perfusion in the ischemic tissue. The overall goal of this study was to deliver therapeutic genes for eNOS and IL-10 to treat the ischemic environment and to characterize at a molecular level the role of eNOS and IL-10 and assess the effect on angiogenic and inflammatory pathways (Figure 1). The specific objectives are: 1) fabrication of an ELP based dual delivery system, 2) determination of a therapeutic dose for eNOS and IL-10, and 3) delivery of eNOS and IL-10 in a hind limb ischemia mouse model to characterize at a molecular level the role of eNOS and IL-10 in angiogenic and inflammatory pathways (Figure 1).

Results

Optimal cross-linking of ELP-based injectable scaffold

An injectable ELP scaffold was fabricated using microbial transglutaminase (mTGase) as a cross-linker (Figure 2A). A 20% ELP scaffold and mTGase of 100 U/g of ELP concentration was found to be the optimal ratio of ELP and mTGase to fabricate the scaffold with a gelation time of 10 min at 37^{o}C. The successful cross-linking of the ELP scaffold was verified by TNBSA (2,4,6-trinitrobenzene sulfonic acid) assay and it was shown that the cross-linked ELP scaffold exhibited 30%±10% reduction in free primary amino groups after cross-linking with mTGase compared to ELP without mTGase (Figure 2B). Cellular cytotoxicity of ELP scaffold was measured using human umbilical vein endothelial cells (HUVECs). Metabolic activity using MTT assay revealed that ELP scaffold cross-linked with mTGase is non-cytotoxic, similar to the control, on tissue culture plastic. The ELP scaffold cross-linked with GTA as a negative control showed higher cellular cytotoxicity than that of ELP/mTGase and the control (Supplementary Figure 2).

Internalization behavior of cells with respect to various sizes of ELP hollow spheres

Various sizes of ELP hollow spheres ranging from 0.1 μm to 10 μm were screened based on optimal loading of pDNA and efficient cellular uptake to be used as a gene delivery depot. Flow cytometry was performed on HUVECS and THP-1 cells treated with FITC-labelled ELP hollow spheres of 0.1, 0.5, 1, and 10 μm sizes. The internalization of ELP hollow spheres into HUVECS did not show any defined pattern, as shown in the case of macrophages, ELP hollow spheres of 0.5, 0.1, and 10 μm size showed more uptake in the HUVECs compared to 1 μm size of hollow spheres (Figure 2C). The activated and non-activated THP1 cells showed a higher uptake of 10 μm ELP HS compared to 0.1, 0.5, and 1 μm sized hollow spheres (Supplementary Figure 1).

Injectable ELP system for dual pDNA delivery

A release study was performed using the ELP-in-ELP injectable system comprising both ELP hollow spheres and the ELP injectable scaffold as gene delivery depot (Figure 2D). Two different sample groups were used for this study: 1) ELP injectable scaffold containing pCMV-GLuc and 2) ELP hollow spheres containing pCMV-GLuc. The release profile of these systems was monitored for 10 days and a cumulative release profile was calculated. The scaffold/polyplex sample group released 20% of *p*DNA by day 1 as compared to ELP hollow sphere/polyplex, which was near to 0%. The scaffold/polyplex group released around 40% of its *p*DNA by day 4 and nearly 90% by the end of 10 days. The ELP hollow sphere/polyplex released a significantly lower percentage of *p*DNA as compared to scaffold/polyplex. The release for ELP hollow sphere/polyplex was only 20% at day 4 and almost 50% by day 10.

Different doses of eNOS and IL-10 and their effect on angiogenesis and inflammation level

An *in vivo* subcutaneous study was performed in C57BL/6 mice to determine a combination of dose for eNOS and IL-10. Nine different treatment groups were tested (Table 1). This *in vivo* subcutaneous study was performed to characterize the degradation profile of the injectable ELP system and also to elucidate an appropriate therapeutic dose to induce angiogenesis and reduce inflammation *in vivo*. The degradation of the ELP scaffold is shown in Supplementary Figure 3. H & E sections of the tissue revealed a 40–50% higher degradation of the scaffold from day 7 to day 14.

Angiogenesis and inflammation analysis of subcutaneous mouse model

Surface and length density of blood vessels were measured from the H & E sections (Images not shown) of the subcutaneous implants of different treatment groups and control (Figure 3A and Supplementary Figure 4). Two different time points, days 7 and 14, were analyzed for this study.

On day 7 the control and IL-10 treatment alone groups showed similar levels of blood vessel density of around 30 mm^2, whereas the eNOS treatment groups showed blood vessel density around 50 mm^2. A trend towards an increase in the blood vessel surface density was found in the eNOS treatment groups. On day 14 the blood vessel density increased up to 139 mm^2 in the eNOS group and was significantly higher than that seen in control groups and IL-10 treatment alone groups (40 up to 55 mm^2). The eNOS doses of both 10 and 20 µg showed significantly enhanced surface density of blood vessels at day 14. The sample treatment group IL-10 (20 µg)/eNOS (20 µg) showed 62% less blood vessel density, while, IL-10 (10 µg)/eNOS (20 µg) showed 30% less blood vessel surface density than eNOS 20 µg alone on day 14 (Figure 3A). Based on the blood vessel surface density data, treatment groups such as ELP alone, IL-10 (10 µg) alone, eNOS (20 µg) alone, and IL10 (10 µg)/eNOS (20 µg) were used to characterize the length density (Supplementary Figure 4).The length densities of all the four treatment groups were found to be similar on day 7. On day 14 both the eNOS treatment groups showed 30–50% higher length density of blood vessels compared to ELP and IL-10 (10 µg) alone. Furthermore, immunostaining of the blood vessels using CD31 supported histological data for vessel density (Supplementary Figure 5). The results showed higher blood vessel density in the treatment groups eNOS (20 µg) and IL10 (10 µg)/eNOS (20 µg).

Inflammation was measured as volume fraction of the infiltrated inflammatory cells from the H & E sections (Figure 3B). At day 7, the volume fraction of inflammatory cells decreased 30% in the case of IL-10 treatment groups compared to ELP alone and eNOS alone treatments. No statistically significant difference was observed between any treatment groups in the amount of inflammatory cells on day 14. CD68 immunostaining, a macrophage marker, showed IL-10 to be effective in reducing the number of macrophages (Supplementary Figures 5).

eNOS and IL-10 expression in the subcutaneous mouse model

The spatio-temporal expression of human eNOS and IL-10 was studied *in vivo*. eNOS and IL-10 protein levels were measured using ELISA. The expression was measured in terms of pg/mg of protein. On day 7 eNOS treated samples showed eNOS expression at the level of 40–60 pg/mg of eNOS. On day 14 the eNOS treated groups showed an increase in eNOS expression level within the range 80–100 pg/mg of protein (Figure 3D).

Similar to eNOS, IL-10 protein expression level was measured for day 7 and day 14. The IL-10 treated group showed expression of IL-10 from the range of 800–1100 pg/mg of protein on day 7. On day 14 reduction in the expression of IL-10 was observed, ranging from 400 to 700 pg/mg of protein (Figure 3C). The control and eNOS alone groups showed an insignificant expression value for both day 7 and day 14.

Inflammatory markers

Nine inflammatory markers comprising of both pro- and anti-inflammatory cytokines were analyzed to determine the pro- and anti-inflammatory cytokines expressed on days 7 and 14 (Figure 3E). Samples from days 7 and 14 were used to extract protein and multiplex ELISA was performed to analyze the expression of different mouse inflammatory markers. TNFα showed no significant difference in their expression level for all the treatment groups. The result is similar for days 7 and 14. IFNγ was found to be expressed more in ELP alone compared to IL-10, eNOS, and IL-10/eNOS treatment groups on day 7, while the eNOS treated group showed significantly lower level of IFNγ than other groups on day 14. IL-1β expression level was significantly less in the eNOS treated group compared to others on day 7 whereas there was no significant difference between all the groups on IL-1β expression level by day 14. IL-10 treatment groups have more expression of mIL-10 on days 7 and 14.

Administration of optimal doses of eNOS and IL-10 in a hind-limb ischemia model

Unilateral hind limb ischemia in a mouse model was successfully generated by permanent ligation of the left femoral artery and vein. Blood perfusion was used as a measure to assess the effect of the treatments on angiogenesis. Blood perfusion was measured after the surgery every week until day 21 using laser Doppler perfusion imaging (LDPI) (Figure 4A), to assess the effect of the treatments on angiogenesis, and is represented as a ratio of perfusion in ischemic limb to non-ischemic limb (Figure 4B). The results showed that eNOS treatment groups had 40–50% more perfusion than IL-10, ELP, and control saline groups. Most of the saline-injected animals showed severely necrotic limbs after 21 days, and ELP and IL-10 alone showed 10–15% of perfusion. The clinical severity of the ischemic limb after treatment was recorded based on the extent necrosis to the foot and discoloration of the limb (Figure 4C). Saline groups showed minimal functional recovery: out of seven animals, three animals showed severely necrotic limbs. The ELP, IL-10, and eNOS alone treated groups showed minimal functional recovery compared to saline. Five out of seven ischemic mice showed functional recovery in the case of eNOS/IL-10 treatment.

Angiogenesis and inflammation levels in the ischemic tissue

Skeletal muscle samples were cryofixed and 5 µm sections were stained with H & E (Images not shown) to measure blood vessel density, which was measured in terms of surface and length density (Figure 5C and Supplementary Figure 6). Day 7 results showed no significant difference between control saline and different treatment groups such as ELP alone, IL-10 (10 µg), eNOS (20 µg), and IL-10 (10 µg)/eNOS (20 µg). By day 21, eNOS and IL-10/eNOS treatment groups showed a 60% increase in surface blood vessel density (Figure 5C). A similar trend was seen in the case of length density measurement, where at day 21 eNOS and eNOS/IL-10 treatment

groups showed a 50% increase in blood length density compared to saline, ELP, and IL-10 alone treatment groups (Supplementary Figure 6).

The volume fraction of inflammatory cells reduced by 50% in the case of IL-10 (10 µg) and 35% for IL-10 (10 µg)/eNOS (20 µg) as compared to saline on day 7. Furthermore, on day 21 the volume fraction of inflammatory cells reduced by 50% for the treatment groups IL-10 (10 µg), IL-10 (10 µg)/eNOS (20 µg) and eNOS alone compared to saline (Figure 5D). These results were further validated using CD31 immunofluorescence staining for endothelial cells (Figure 5A) and CD68 (Figure 5B) for inflammatory cells. CD68 immunostaining data showed that overall macrophages are fewer for IL-10 treated groups for days 7 and 21. CD31 staining showed increased blood vessels in the eNOS treated groups on day 21.

Human eNOS expression in the ischemic tissue was analyzed for different treatment groups by ELISA (Figure 4E). It was observed that eNOS treated groups such as IL-10 (10 µg)/eNOS (20 µg) and eNOS (20 µg) significantly up-regulated expression of eNOS at days 7 and 21 compared to other groups. Also, at day 21 the expression level of eNOS for eNOS treated groups was seen to be significantly more than day 7 expression. A similar trend was found in the case of IL-10 expression, where IL-10 treatment groups such as IL-10 (10 µg) and IL-10 (10 µg)/eNOS (20 µg) showed a significant up-regulation of IL-10 compared to other groups by days 7 and 21. Also, expression level decreased significantly from day 7 to day 21 (Figure 4D).

eNOS and IL-10 and their regulation of angiogenesis and inflammation at the molecular level

RT-PCR was performed to analyze gene expression of major angiogenic and inflammatory factors. On day 21, eNOS treatment groups showed upregulation of FGF1, PDGFB, VEGFA, and VEGFB (Figure 6A). The eNOS alone treated group was found to have significantly (10–18-

fold) increased expression of FGF1 over that of IL-10/eNOS and 3–4-fold from IL-10 and ELP groups on day 21. Similarly, the eNOS alone treated group was seen to have a significant increased expression of PDGFB over that of ELP and IL-10/eNOS groups at day 21 (Figure 6A). In the case of VEGFA the up-regulation at day 21 was significantly higher compared to ELP, IL-10, and eNOS/IL-10 treatment groups. Furthermore, VEGFB expression in the eNOS alone treatment significantly increased: around 4–5-fold more than ELP, 2-fold more than IL-10, and 5-fold more than that of eNOS/IL-10 groups.

The expression of inflammatory markers IFNγ, IL-4, TNFα, and IL-1β was analyzed (Figure 6B). The IL-10/eNOS treatment group showed 2–6-fold higher up-regulation of IL-4 on day 21 from its earliest time point of day 7 (Figure 6B). Also, IL-4 expression level was significantly higher in the case of IL-10/eNOS group compared to ELP and IL-10 alone. No statistically significant difference was detected for IL-1β, TNFα and IFNγ for any of the groups and time points.

Moreover, the factors that showed higher expression compared to day 7 expression level were FGF1, SerpinF1, VEGFA, VEGFB, and PDGFB. A statistically significant (2–10–fold) increase in expression level of SerpinF1 was seen from day 7 to day 21 for the eNOS treated groups such as eNOS and IL-10/eNOS (Figure 6A). FGF1 was found to have a significantly increased expression level from day 7 to day 21 for eNOS and IL-10 treatments except for scaffold and eNOS/IL-10 treatment groups (Figure 6A). Also, a significant increase in expression of PDGFB from day 7 to day 21 was seen in the eNOS alone group. Furthermore, VEGFA showed significant (2–12-fold) up-regulation by 21 days in all the groups except the IL-10/eNOS group (Figure 6A). Also, a significantly increased expression of VEGFB was seen from day 7 to day 21 for both IL-10 and eNOS alone treatment groups (Figure 6A).

Discussion

In this study, an injectable ELP delivery system was designed to deliver therapeutic plasmids encoding IL-10 and eNOS. The aims of the study were to reduce the early onset of inflammation followed by stimulation of angiogenesis in ischemic tissue. This approach necessitated a delivery vehicle that spatio-temporally releases two different genes. Previous studies have reported the fabrication of ELP hollow spheres of various sizes and their use as a gene depot [19]. However, screening various sizes of ELP hollow spheres was necessary to characterize internalization pattern in endothelial cells and macrophages. These cells were chosen for the study as they are found abundantly in ischemic tissue [22, 23]. This screening was performed to find a suitable size of ELP hollow sphere that can be used to load *p*DNA inside with minimal internalization into both endothelial cells and macrophages. The FACS study revealed that in HUVECs 0.1 and 0.5 μm spheres were internalised more than 1 μm spheres, suggesting size dependent uptake in this cell type. Size dependent uptake of the spheres within the cells has been previously reported in the literature, however macrophages are known to engulf bigger particles [24, 25]. It was found that ELP hollow spheres of 10 μm were engulfed by both activated and non-activated macrophages compared to 1, 0.5, and 0.1 μm ELP hollow spheres. Thus, considering the amount of *p*DNA that can be loaded within ELP hollow spheres without internalization by macrophages and endothelial cells, 1 μm ELP hollow sphere was chosen to be the gene depot. The previous study performed on size and loading efficiency showed that there was no significant difference between various sizes of spheres for their *p*DNA loading efficiency. However, the larger the ELP hollow sphere, the more *p*DNA can be loaded for a spontaneous release of the *p*DNA.

An injectable scaffold was fabricated so that ELP hollow spheres and injectable scaffold can be combined to deliver dual therapeutic genes IL-10 and eNOS. The biomaterial system used was

an ELP scaffold which would be injectable and gel *in situ* without causing any cytotoxicity. In this study, the ELP injectable scaffold was fabricated by using mTGase as the cross-linker. mTGase is an enzyme of bacterial origin and catalyzes the acyl transfer reaction between an ε-amino group of lysine residue and a γ-carboxamide group of glutamine residue by introducing covalent cross-links between proteins, peptides, and various primary amines [26]. Additionally, its ease of production and Ca^{2+} independent activity make it more suitable than tissue TGase [26]. mTGase catalyzes the acyl transfer reaction between glutamine and lysine residues present in the cross-linking domains of ELP. The TNBSA assay showed a decrease in the amount of free amino groups in the mTGase and GTA cross-linked groups. The number of free amino groups available was reduced greatly after cross-linking with GTA compared to mTGase. This further explains the role of mTGase as a mild cross-linker leaving free amino groups in the scaffold. These free amino groups help the scaffold to hold negatively charged *p*DNA or neutrally charged polyplexes with the help of an electrostatic interaction, and thus were released only by treating with an enzyme such as elastase. Free amino groups played an important role in binding *p*DNA complexes, which are released only under the action of protease and elastase enzymes [19]. The release data showed that the dual delivery system released *p*DNA with the treatment of elastase, which is abundant in the ischemia area [27]. Also, *p*DNA was released faster from the scaffold than from ELP hollow spheres. Thus, this system as designed was able to load two different genes at the same time and deliver them spatio-temporally.

To further validate the use of the ELP injectable system *in vivo* and to determine a therapeutic dose of eNOS and IL-10, a subcutaneous study was performed in the mouse model. ELISA data showed higher expression of eNOS and IL-10. Day 7 showed more IL-10 expression, and it decreased at day 14. In contrast, eNOS expression increased by day 14, while at day 7 there was

reduced expression compared to day 14. The pattern of expression of eNOS and IL-10 is temporal and can be correlated to the *in vitro* release of the ELP injectable system. In the ELP injectable system IL-10 *p*DNA was loaded inside the scaffold and eNOS *p*DNA inside the ELP hollow spheres and thus with the initial degradation of the scaffold, IL-10 was released earlier than eNOS. This led to the higher expression of IL-10 by day 7, while for eNOS the highest expression was by day 21. A highest dose of 20 µg and lowest of 10 µg were chosen for the *p*DNA to perform the dose study. Combinations of the two genes including all the doses were used to do the dosage study.

In total, nine treatment groups were tested in subcutaneous mouse model. The histology data for angiogenesis and inflammation were in accordance with the IL-10 and eNOS expression data. By day 14 there was a difference between groups with and without eNOS in the amount of vessel and length density. On the other hand, by day 7 a reduction in the volume of inflammatory cells could be noticed with IL-10 treatment groups as the IL-10 released from the scaffold reduced the minor inflammation caused by implantation. However, by day 14 there was no big difference in the level of inflammatory cells between all the groups. The reason might be that the subcutaneous mouse model used in this study is not a perfect model to study inflammation for a longer period. The angiogenesis data obtained from the stereology showed that eNOS treatment groups such as eNOS (20 µg) and IL-10 (10 µg)/eNOS (20 µg) indicated comparatively more blood vessel density than eNOS in combination with a bigger dose of IL-10 such as IL-10 (20 µg)/eNOS (20 µg) and IL-10 (20 µg)/eNOS (10 µg). This might be due to an inhibitory effect of IL-10 on angiogenesis [28], when used at a higher dose as seen here. The eNOS at a dose of 20 µg showed higher surface and length density of blood vessels, and in a combination with IL-10 µg reduced the inflammation level without inhibiting angiogenesis. Thus, the treatment group

IL-10 (10 µg)/eNOS (20 µg) was chosen for the ischemic study. Moreover, blood vessel surface density was found to have a correlation with the length density in the IL-10/eNOS treatment group. The correlation study showed an increase in surface density and length density with an increase in eNOS expression.

The immunostaining for CD68 and CD31 was in accordance with the histology data for macrophages and vessel density data respectively. The CD68, a universal marker for a wide array of macrophages, was found to be reduced with the treatment of IL-10 and so eNOS treated showed more blood vessel density stained with CD31. The dose study further assessed the combined effect of IL-10 and eNOS. The IL-10/eNOS treatment groups showed an apparent decrease in the level of inflammatory cells by day 7 and an increase in blood vessel density by day 14. But with an increase in dose of the IL-10 the level of blood vessel density decreased. This inhibitory effect on angiogenesis might be because of the antiangiogenic activity of IL-10.

Ischemic study was performed using a mouse model of unilateral ischemia. There were five groups: saline, eNOS (20 µg), IL-10 (10 µg), eNOS (20 µg)/IL-10 (10 µg), and ELP alone. The treatment groups that showed higher blood perfusion measured using LDPI were in groups treated with eNOS. Saline showed a higher amputation rate. ELP and IL-10 (10 µg) showed minimal blood perfusion. The histological data were in accordance with the LDPI as surface and length density of blood vessels were significantly higher in the case of eNOS treated samples. The correlation study showed a decrease in inflammation with an increase in IL-10 expression in one of the treatment group. This was further proved by immunostaining with CD31. ELISA test for eNOS showed a similar pattern as seen in the case of subcutaneous dose study. eNOS was expressed significantly by day 21 and thus a higher blood perfusion was seen by three weeks time. eNOS treatment groups enhanced protein expression of eNOS much more than its

endogenous level (<50 ng/mg of protein) in skeletal muscle [29, 30]. Also, the expression level of eNOS was very similar to that observed in lipoplex mediated eNOS delivery. Similarly, IL-10 treatment groups enhanced the level of IL-10 protein expression in the skeletal muscle, which was significantly higher than previously reported (<100 pg/mg of protein) [31]. eNOS is a major proangiogenic factor and induces angiogenesis by mobilization of vascular endothelial cells and endothelial progenitor cells. eNOS produces NO, which acts as a signaling molecule in the angiogenic pathway [32]. On the other hand, IL-10 acts on proinflammatory cytokines and macrophages to reduce the inflammation level in the ischemic tissue [12]. IL-10 containing treatment groups significantly reduced the amount of inflammatory cells as per the stereological analysis of the H & E sections. This was further proved by CD68 immunostaining of macrophages. The ELISA data showed earlier release of IL-10 and thus a significant reduction in the number of inflammatory cells was seen in the IL-10 treatment groups. IL-10 in combination with eNOS showed increased vascularization of the ischemic tissue with reduced inflammation by three weeks.

Furthermore, a mechanistic study was performed to elucidate the cross-talk of IL-10 and eNOS in the ischemic muscle with respect to inflammation and angiogenesis. Ischemic angiogenesis, as mentioned above, is regulated by several angiogenic factors, the major factors being VEGF, PDGFB, bFGF [7-9, 13]. The eNOS treatment group induced up-regulation of VEGFA and B, potent angiogenic cytokines, which also increases vascular permeability with the help of nitric oxide. Furthermore, eNOS treatment groups also showed an increasing level of serpinF1, an anti-angiogenic factor. SerpinF1 is known to inhibit the migration and proliferation of endothelial cells induced by VEGF [33], and then further inhibits angiogenesis by interacting with specific cell surface receptors. This anti-angiogenic activity of serpinF1 is critical for the regulation of

angiogenesis. Another major proangiogenic factor up-regulated with the treatment of eNOS is PDGFB, which helps in stabilization of newly formed blood vessels [34, 35]. eNOS thus up-regulates major proangiogenic factors such as bFGF, VEGF(A and B), and PDGFB to induce angiogenesis. It is known that a short exposure of PDGFB and FGF-2 in the ischemic tissue would be sufficient to establish stable and functional vessels [6]. This shows the role of eNOS in establishing a stable and functional vascular network through up-regulation of bFGF and PDGFB. Also, a decrease in the expression of these specific growth factors can be noticed in the presence of IL-10, suggesting an inhibitory effect of IL-10 on angiogenesis. ELP scaffold itself helps in up-regulation of these major growth factors, but the effect is less than that with eNOS alone. Ischemia leads to damage of the local tissue and thus is a site for inflammation. One of the major anti-inflammatory cytokine is: IL-4 [36, 37]. No significant effect of IL-10 alone was found on IL-4 factor, whereas IL-10/eNOS treatment group showed an enhanced level of IL-4, anti-inflammatory cytokine. Several studies have proposed that maintaining a balance between the proangiogenic and antiangiogenic factors is critical for the regulation of angiogenesis [38-40]. Thus, use of a combination of eNOS and IL-10 can provide a balance in angiogenesis by inducing a differential expression of proangiogenic and anti-angiogenic factors in the ischemic tissue. The results are briefly summarized in Figure 8.

In summary, this study reported the fabrication of an injectable ELP based system to deliver IL-10 and eNOS in a spatio-temporal manner. The injectable system was assembled by using ELP hollow spheres and injectable ELP scaffold as two separate gene delivery depots. The results showed that 1 μm ELP hollow spheres when used as a depot are less internalized into the cells predominantly found in an ischemic tissue, such as endothelial cells and macrophages. The delivery system showed a spatio-temporal release of two different genes. A dose of eNOS (20

μg) and IL-10 (10 μg) reduced inflammation level and increased angiogenesis in both subcutaneous and ischemic mouse models. The dosage study also showed an inhibitory effect of IL-10 on angiogenesis, especially when a high dose of 20 μg was used. RT-PCR study showed that eNOS induced major proangiogenic factors by weeks 1 and 3 and helped in vascularization of the ischemic tissue. And along with IL-10, it reduces the early onset of inflammation level by inhibiting major proinflammatory cytokines. Although use of IL-10 reduced the angiogenic potential of ischemic tissue, later this was compensated by eNOS induced up-regulation of proangiogenic factors.

Overall, the study was designed to show a holistic approach to the treatment of ischemic conditions rather than focusing only on angiogenesis, and to elucidate an underlying mechanism between inflammation and angiogenesis by using eNOS and IL-10. The study showed the importance of a dose study before any gene therapy, and opens up opportunities to do further preclinical studies in larger animals before moving to clinical trials. Additionally, the ELP-based injectable system shows potential to be used in any disease model for gene delivery.

Materials and Methods

Polystyrene (PS) beads of 0.1, 0.3, 10 μm, sulphuric acid, tetrahydrofuran (THF), DNase free water, agarose, sodium chloride, sodium acetate, sodium bicarbonate, poly-D-glutamic acid (PGA), glutaraldehyde, Dulbecco's modified Eagle's medium (DMEM) with L-glutamine, Hank's balanced salt solution (HBSS), phosphate buffer saline (PBS), bovine serum albumin (BSA), and fetal bovine serum (FBS) were purchased from Sigma-Aldrich. PS beads of diameter 0.5 and 1 μm were obtained from GENTAUR. Quant-iT^{TM} PicoGreen$^{®}$ dsDNA kit, alamarBlue$^{®}$, fluorescein isothiocyanate (FITC), and trinitrobenzene sulfonic acid (TNBSA) were obtained from Thermo Scientific. Gaussia luciferase (pCMV-GLuC) was purchased from New England

BioLabs®. Ca^{2+}-independent microbial transglutaminase (mTGase) was purchased from Activa®WM. CM52 cation exchange resin was purchased from Whatman®, and transglutaminase (TGase) colorimetric microassay kit was purchased from Covalab. EP20-24^4 was provided by Elastin Specialties and SuperFect® was purchased from QIAGEN. HUVECS and endothelial growth basal medium (EBM-2) along with the kits were obtained from Lonza, and human acute monocytic leukemia cell line (THP1) was obtained from ATCC. Human eNOS and IL-10 ELISA kit were from R&D Systems. Multiplex cytokine measurement kit was from Meso Scale Discovery and RT-PCR array and kits were from QIAGEN.

EP20-244 polypeptide expression and purification

EP20-24^4 relates to the recombinant ELP with exons 20-21-23-24-21-23-24-21-23-24-21-23-24 found in the human aortic elastin, and was expressed and purified as reported previously [41]. ELP of 94% purity was obtained from Elastin Specialties, Canada.

Purification of mTGase

Ca^{2+}-independent mTGase was purified as previously described [19]. Briefly, the mTGase enzyme sample was dissolved in 20 mM sodium acetate buffer (pH 5.8) at a concentration of 500 mg/ml and added to a glass column (1.5 × 30 cm) containing CM52 cation exchange resin pre-equilibrated with the above buffer at a flow rate of 2 ml/min. The sample was washed with two column volumes of the same buffer and eluted by a gradient of 10 column volumes from 0 to 0.5 M sodium chloride. The samples were analyzed at 280 nm for eluted protein. Pooled fractions were concentrated, dialyzed into PBS, and analyzed for enzyme activity using the transglutaminase colorimetric micro assay kit and purified guinea pig TGase (control) with known units of enzyme activity as standard (where 1 unit will catalyze the formation of 1 µmole

of hydroxamate at pH 6.0 at 37°C using L-glutamic acid-monohydroxamate as the standard). Typical activity recovered was in the range of 0.5 U/mg mTGase.

Fabrication of hollow spheres

ELP hollow spheres were fabricated using a template-based method [24, 42, 43] as described previously [19]. Briefly, the fabrication method includes three steps: coating, cross-linking, and dissolution of the PS core to obtain hollow ELP spheres. Monodispersed PS beads were sulfonated to create a negative surface charge on the sphere. These sulfonated PS beads were then used as a template. ELP of ~35 kDa was used to coat the sulfonated PS beads in PBS. The coated beads were then cross-linked using mTGase. Finally, PS beads were dissolved using THF to obtain hollow spheres.

Fabrication of *in situ* injectable scaffold

A scaffold capable of gelling *in situ* was fabricated using ELP and mTGase. Briefly, various concentrations of ELP and mTGase were used for fabrication of the scaffold. ELP with 2%, 5%, and 10% (weight/volume) were dissolved in water and with 25, 50, and 100 U of mTGase (U/g of ELP concentration) with several combinations. The ELP/mTGase solutions were incubated in a water bath at 37^{o}C.

Gelation was characterized at different time points ranging from 5 to 30 min. The combination of ELP and mTGase concentrations (10% of ELP and 100 U of mTGase) gelling at 10 min was further characterized for its cross-linking and cell viability.

TNBSA assay for cross-linking

The cross-linking of ELP hollow spheres with mTGase has been characterized previously [19], and cross-linking of an ELP scaffold with mTGase was performed similarly. TNBSA is a hydrophilic modifying reagent for the detection of primary amines in samples containing amino

acids, peptides, or proteins [44]. It reacts readily with the N-terminal amino groups of amino acids in aqueous solution at pH 8 to produce a yellow color. The colored derivatives are detected at 335–345 nm. ELP, both with and without treatment of mTGase, was used for the assay. mTGase concentrations of 20, 50, and 100 U/g of ELP were used to cross-link ELP. In addition, ELP cross-linked with glutaraldehyde was used as a positive control. For this particular experiment, the cross-linked ELP scaffolds were hydrolyzed in 1N HCl to hydrolyze into a solution. The hydrolyzed ELP solution was then used for the assay.

Cell viability

MTT assay was performed to quantify the cell viability of HUVECS in contact with the scaffold. Injectable ELP scaffolds were fabricated in a 96 well tissue culture plate. Briefly, 100 µl mixture of ELP and mTGase was plated in several wells of a 96 well plate and incubated at 37°C for 10 min. The ELP scaffolds were then equilibrated for 24 h using EGM-2 medium. The medium was discarded after 24 h of equilibration. HUVECs were harvested using 0.25% of trypsin-EDTA. Finally, HUVECs were seeded at cell density of 1×10^4 cell/well for 24 h. The culture medium was replaced with fresh medium after 24 h of seeding. HUVECs on tissue culture plates were kept as a positive control and glutaraldehyde cross-linked scaffolds as a negative control. MTT assay was used to assess the cell viability. The scaffolds seeded with HUVECS, along with controls, were washed with HBSS and replaced with 200 µl of fresh MTT (0.5 mg/ml) solution. This was followed by 4 h incubation at 37°C in 5% CO_2. After the required incubation this MTT solution was decanted carefully and 200 µl dimethyl sulfoxide (DMSO) was added to dissolve the formed formazan crystals. The absorbance of the solution was measured at 595 nm on a microplate reader (VarioskanFlash-4.00.53).

Propagation of plasmid and isolation

Plasmid pCMV-GLuc, human eNOS (heNOS) and human IL-10 (hIL-10) plasmids were transformed into XL1-Blue (Stratagene) competent cells and selected twice in ampicillin antibiotic containing LB broth and on LB agar plates. Plasmid expansion was performed as recommended in the Giga-Prep (Qiagen) protocol and isolated using that kit. Plasmid purity was confirmed by UV spectroscopy (NanoDrop™ ND1000 Spectrophotometer, Thermo Scientific) and gel electrophoresis.

Formulation of polyplex

Polyplexes were prepared using commercially available SuperFect® and pCMV-GLuc, heNOS, and hIL-10 plasmids in PBS pH 7.4. The weight–weight ratios of SuperFect® and plasmids were optimized to 20:1.

***In vitro* internalization study of ELP hollow spheres using flow cytometry**

HUVECs and THP1 cells were grown in T25 tissue culture flasks for flow cytometry studies. HUVECs were cultured using EBM-2 medium and THP1 non-adherent cells were cultured in RPMI-1640 supplemented with 10% FBS and 1% P/S and L-glutamine at 37ºC in humidified 5% CO_2. Culture of adherent macrophages from THP1 monocytes was achieved by using phorbolmyristate acetate (PMA) in a differentiation media and were activated using TNFα. Briefly, the THP1 cells at a density of 800,000–1,000,000 cells/ml were cultured on tissue culture plates in an RPMI-1640 differentiation medium containing 5 g/L glucose, 1% P/S and L-glutamine, and PMA at a final concentration of 100 ng/ml for 24 h.

For the flow cytometry analysis HUVECs and activated and non-activated THP1 were incubated with FITC labeled ELP hollow spheres of 0.1, 0.5, 1, and 10 μm sizes at a concentration of 50μg/ml concentration. After the desired incubation time, cells were trypsinized and resuspended

in a buffer (1% BSA in PBS). Cells were then analyzed using flow cytometry for internalization efficiency.

***In vitro* release study**

In vitro dual release studies of *p*DNA were performed on the injectable ELP-in-ELP (ELP hollow spheres embedded within ELP scaffold) system. The injectable system comprised scaffold and 1 µm ELP hollow spheres which were loaded separately with pCMV-GLuc. Two different samples of ELP-in-ELP were prepared, where one of the group was carrying *p*DNA in the scaffold and another group in the ELP hollow spheres. The systems were tested for the release of *p*DNA with and without treatment of enzyme elastase. Briefly, 250 mg samples of 1 µm ELP hollow spheres were re-suspended in 300 µl of PBS and polyplexes containing 20 µg of *p*DNA were added. This mixture was then agitated for 12 h at room temperature. The suspension was centrifuged at 13,000g and the ELP hollow sphere/polyplex complexes were washed four times with MilliQ purified water. The ELP hollow sphere/polyplexes were then mixed with ELP solution containing mTGase and incubated at 37°C to form a gel encapsulating the ELP hollow spheres. In another sample, ELP solution 10% (w/v) was mixed with mTGase and 20 µg pCMV-GLuc polyplexes along with the ELP hollow spheres without *p*DNA. Both the samples were incubated in PBS with elastase at 37°C for 10 days to characterize their release profile. The supernatants were collected and quantified using PicoGreen® assay. Briefly, the supernatants with polyplexes were treated with high concentration (10 mg/ml) of poly-D-glutamic acid (PGA) for 30 min to break the SupeFect/*p*DNA complex bound in order to get free *p*DNA. Finally, this free *p*DNA was used to quantify the release pattern from the scaffold.

***In vivo* studies**

The ability of an injectable ELP system to deliver two therapeutic genes of interest (eNOS and IL-10) and their therapeutic doses was investigated in an *in vivo* subcutaneous mouse model. Subsequently, a unilateral hind limb ischemic model was created to test the effect of human IL-10 and eNOS expression in an ischemic condition. Male C57BL/6 mice 10 weeks old were used for this study. All experimental procedures and protocols were approved by the Ethics Committee of the National University of Ireland, Galway under the license (B100/4131) granted by the Department of Health and Children, Dublin, Ireland. Mice were housed in groups of three per cage under controlled temperature and humidity conditions. They were fed a regular chow diet and had access to water.

Subcutaneous dose response study

Animals were anaesthetized using intra-peritoneal injection of ketamine (80–100 mg/kg) with xylazine (10 mg/kg). The skin overlying the scruff and back of each animal was shaved. The treatments were randomised injected in four different places in each mouse. The total sample volume was kept at 100 µl, with different formulations of eNOS (10 and 20 µg) and IL-10 (10 and 20 µg) encapsulated in ELP hollow spheres and scaffolds respectively. The total number of treatment groups was nine, including the control group of ELP scaffold/hollow spheres alone. Two different time points, days 7 and 14, were taken to study both inflammation and angiogenesis, with six animals for each treatment group. The animals were sacrificed at days 7 and 14 and the tissue samples were harvested. Each tissue sample was dissected into two halves. One half of the sample was fixed with 4% formaldehyde for histological and immunohistochemical analysis and the other half was divided again into two halves and stored at – 80^{o}C for protein and mRNA analysis.

Hind limb ischemic study

Mice were anaesthetized using a combination of ketamine (80–100 mg/kg) and xylazine (10 mg/kg) administered intraperitoneally. The limbs of the mice were shaved and sterilized using iodine before the surgery. The femoral artery was exposed by performing an incision in the skin overlying the middle portion of the hind limb of each mouse (unilateral). Left femoral artery and vein were ligated proximal to the profunda femoris and excised. The overlying skin was then closed using a surgical suture. Animals were closely monitored until full recovery from anesthesia. Laser Doppler perfusion imaging (LDPI) was performed before and after surgery to assess the perfusion level in the ischemic limbs. An ELP injectable system containing IL-10 and eNOS was injected intramuscularly. There were five treatment groups in total, including control saline and empty scaffold/empty hollow sphere alone. Blood perfusion level was monitored over different time points (1, 2, and 3 weeks) using LDPI. Animals were housed separately post-surgery under controlled temperature and humidity conditions. Postoperative buprenorphine was administered for analgesia. Clinical signs manifested due to poor or occluded blood flow to the limb was semi-quantitatively assessed by gross examination of the degree of necrosis and ambulation in the left limb until day 21 [45, 46]. A modified four-point scale was used to assess the severity of the induced ischemia. 1= plantar flexion, mild discoloration 2= No plantar flexion, mild discoloration 3= No plantar flexion, moderate to severe discoloration 4= necrosis or auto-amputation of toes (2 or more). Animals were sacrificed at different time periods (weeks 1 and 3) with CO_2 asphyxiation. The tissue sections were processed for histological evaluation and protein and mRNA expression analysis as described previously.

Histology and immunohistochemistry

Samples from subcutaneous implants were paraffin embedded whereas for ischemic study tissue samples were frozen embedded using cryo-OCT compound. Blocks were cut into sections of 5µm thickness. Nine sections were cut from each block from three different depths with 100µm intervals. Slides were stained with H & E using standard protocol. The images for identification of inflammatory cells and blood vessels were taken at 400× magnification in the beginning for consistency.

Identification of blood vessels was confirmed by immunofluorescence staining of the endothelial cell membrane marker CD31 using standard protocols. Briefly, tissue sections from the paraffin embedded samples were deparaffinized and processed through a gradient from 100% ethanol to 50% and finally in water. Furthermore, enzymatic antigen retrieval was carried out at 37^{o}C using 1X proteinase K solution in TE buffer (50 mM Tris Base, 1 mM EDTA, pH 8.0). The primary antibody used was polyclonal rabbit anti-CD31 (Abcam, Dublin, Ireland) (1:100 in 0.01 M PBS containing 1% BSA, 0.1% cold fish skin gelatin), incubated overnight at 4^{o}C. Blocking buffer was added to three slides as negative control. Secondary goat anti-rabbit IgG Alexa Fluor® 488 (1:400 in 0.01 M PBS, Invitrogen, Ireland) was applied for 45 min at room temperature, followed by DAPI as a counterstain.

Identification of macrophages was confirmed by immunohistochemistry using a standard protocol. Briefly, enzymatic antigen retrieval was carried out at 37 ^{o}C using 1X proteinase K (20 mg/ml) solution in TE buffer (50 mM Tris Base, 1 mM EDTA, pH 8.0). The primary antibody used was rabbit polyclonal macrophage CD 68 (Abcam, Dublin, Ireland) (1:100 in 0.01 M PBS containing 1% BSA, 0.1% cold fish skin gelatin), with overnight incubation at 4°C. Blocking buffer was added to three slides as negative control. Secondary goat anti-rabbit IgG Alexa Fluor®

488 (1:400 in 0.01 M PBS, Invitrogen, Ireland) was applied for 45 min at room temperature, followed by DAPI as a counterstain.

Stereology

Six fields of view of the H & E stained slides were captured at 400× magnification. The volume fraction of inflammatory cells was measured using a 192-point grid. The surface density and length density of blood vessels were measured using a cycloidal line grid.

Inflammation

Volume fraction (V_V) is a relative parameter best estimated by point counting [47]. The number of neutrophil- and macrophage-cell nuclei intersecting grid points was counted (P_P). This number was divided by the total number of grid points for each field of view (P_T), and a cumulative volume fraction of inflammatory cells was calculated for the six fields of view on each section. The following formula was used to calculate volume fraction of inflammatory cells.

$$V_V = \frac{P_p}{P_T} \qquad (1)$$

Angiogenesis

A cycloidal grid of 40 μm radius was overlaid on each field of view [47]. The grid consisted of six test lines, each comprising 10 cycloid arcs. Therefore, the total length (L_T) of cycloid arcs was 2400 mm. The number of times a blood vessel intersected (I) an arc was counted, and the following standard equation was used to measure the surface density (S_V).

$$S_V = 2 \times \frac{I}{L} \qquad (2)$$

Length density of blood vessels was measured by rotating each captured field of view by 90°. The cycloidal grid was placed in the same orientation as described above. The grid now consisted of eight test lines, each comprising eight cycloid arcs of radius 40 μm. The total length of test line (L_T) was therefore 2560 mm. The number of intersections between blood vessels (I_L) and test line was counted, and the length density (Lv) of blood vessels was calculated using the following equation, where T_S is the thickness of the section.

$$L_T = \frac{2 \times I_L}{T_S} \quad (3)$$

This distance is critical to determine the efficiency of new blood vessels, as it measures the zone of diffusion around blood vessels.

Quantification of eNOS and IL-10 level

Protein analysis was conducted on tissue homogenates using human IL-10 and eNOS ELISA kit from R&D Systems. Briefly, tissue samples were suspended in Tissue Extraction Reagent (Sigma, Dublin, IE) at 20 mg/mL. The samples were incubated for 5 min at 4^{o}C and then homogenized using a Tissue Ruptor (Qiagen, Crawley, UK). Homogenates were centrifuged at 10,000g for 10 min to remove particulates. The IL-10 and eNOS content in the supernatant was then analyzed and normalized to the total protein content, as analyzed using the bicinchoninic acid assay.

Multiplex cytokine measurements

A mouse inflammatory cytokine multiplex array (Meso Scale Discovery, Gaithersburg, MD) was used to analyze the relative levels of a variety of inflammatory cytokines. Briefly, tissue lysates extracted as described above were added to plates carrying antibodies for interferon gamma

(IFN-γ), interleukin 1β,-10 (IL-1β, IL-10), tissue necrosis factor alpha (TNFα). The plate was then imaged with a SECTOR® Imager 2400 (Meso Scale Discovery, Gaithersburg, MD).

RT-PCR Analysis

RNA was isolated using RNeasy® Micro Kit (QIAGEN), following the manufacturer's protocol. Briefly, cells were homogenized by Trizol and then phase separated using chloroform. The quantity of RNA isolated was checked spectrophotometrically using a NanoDrop. The quality was checked using Agilent RNA. The isolated RNA was first reverse transcribed using Reverse Transcription System (QIAGEN). The cDNA thus obtained was then used for real time PCR reaction (ABI StepOnePlus™ Real-Time PCR System, software v2.1). The PCR array was designed (QIAGEN) for 9 genes: fibroblast growth factor 1(FGF1), platelet derived growth factor B (PDGFB), serpinF1, vascular endothelial growth factor A and B (VEGFA and VEGFB), IFN-γ, IL-1β, IL-4, TNFα. with their specific primers, and RT^2 SYBR Green Mastermix (QIAGEN) was used under standard conditions to perform the RT-PCR. *18s rRNA* was used as a reference gene to normalize the qRT-PCR data.

Statistics

Statistical analyses were performed using GraphPad Prism® Version 5 (USA). All bar charts represent mean ± standard deviation. Data were compared using One-way ANOVA with post-hoc Tukey's multiple comparisons test. $P < 0.05$ was considered statistically significant (*).

Acknowledgements

This work was supported by Science Foundation Ireland under grant no. 07/SRC/B1163. The authors would like to thank Elastin Specialties, Canada for providing ELP. We are also thankful to Mr. Anthony Sloan for his editorial support and Mr. Maciej Doczyk for his assistance in graphic illustrations.

References

[1] Ouriel K. Peripheral arterial disease. Lancet 2001;358:1257-64.

[2] Tulsyan N, Ouriel K, Kashyap VS. Emerging drugs in peripheral arterial disease. Expert Opin Emerg Drugs 2006;11:75-90.

[3] Eliason JL, Wakefield TW. Metabolic consequences of acute limb ischemia and their clinical implications. Semin Vasc Surg 2009;22:29-33.

[4] Lavu M, Gundewar S, Lefer DJ. Gene therapy for ischemic heart disease. J Mol Cell Cardiol 2011;50:742-50.

[5] Thomas D, Fontana G, Chen X, Sanz-Nogues C, Zeugolis DI, Dockery P, et al. A shape-controlled tuneable microgel platform to modulate angiogenic paracrine responses in stem cells. Biomaterials 2014;35:8757-66.

[6] Cao R, Brakenhielm E, Pawliuk R, Wariaro D, Post MJ, Wahlberg E, et al. Angiogenic synergism, vascular stability and improvement of hind-limb ischemia by a combination of PDGF-BB and FGF-2. Nat Med 2003;9:604-13.

[7] Cao Y. Molecular mechanisms and therapeutic development of angiogenesis inhibitors. Adv Cancer Res 2008;100:113-31.

[8] Cao Y. Tumor angiogenesis and molecular targets for therapy. Front Biosci 2009;14:3962-73.

[9] Cao Y. Angiogenesis: What can it offer for future medicine? Exp Cell Res 2010;316:1304-8.

[10] Khawaja FJ, Kullo IJ. Novel markers of peripheral arterial disease. Vasc Med 2009;14:381-92.

[11] Swain MG, Appleyard CB, Wallace JL, Maric M. TNF-alpha facilitates inflammation-induced glucocorticoid secretion in rats with biliary obstruction. J Hepatol 1997;26:361-8.

[12] Moore KW, de Waal Malefyt R, Coffman RL, O'Garra A. Interleukin-10 and the interleukin-10 receptor. Annu Review Immunol 2001;19:683-765.

[13] Cao Y. Positive and negative modulation of angiogenesis by VEGFR1 ligands. Sci Signal 2009;2:re1.

[14] Crystal RG. Transfer of genes to humans: early lessons and obstacles to success. Science 1995;270:404-10.

[15] Shimamura M, Nakagami H, Taniyama Y, Morishita R. Gene therapy for peripheral arterial disease. Expert Opin Biol Ther 2014;14:1175-84.

[16] Felgner PL, Gadek TR, Holm M, Roman R, Chan HW, Wenz M, et al. Lipofection: a highly efficient, lipid-mediated DNA-transfection procedure. Proc Natl Acad Sci USA 1987;84:7413-7.

[17] Lee H, Jeong JH, Park TG. PEG grafted polylysine with fusogenic peptide for gene delivery: high transfection efficiency with low cytotoxicity. J Control Release 2002;79:283-91.

[18] Thomas CE, Ehrhardt A, Kay MA. Progress and problems with the use of viral vectors for gene therapy. Nat Rev Genet 2003;4:346-58.

[19] Dash BC, Mahor S, Carroll O, Mathew A, Wang W, Woodhouse KA, et al. Tunable elastin-like polypeptide hollow sphere as a high payload and controlled delivery gene depot. J Control Release 2011;152:382-92.

[20] Kim W, Chaikof EL. Recombinant elastin-mimetic biomaterials: Emerging applications in medicine. Adv Drug Deliv Rev 2010;62:1468-78.

[21] Nettles DL, Chilkoti A, Setton LA. Applications of elastin-like polypeptides in tissue engineering. Adv Drug Deliv Rev 2010;62:1479-85.

[22] Brechot N, Gomez E, Bignon M, Khallou-Laschet J, Dussiot M, Cazes A, et al. Modulation of macrophage activation state protects tissue from necrosis during critical limb ischemia in thrombospondin-1-deficient mice. PLoS One 2008;3:e3950.

[23] Dai Q, Thompson MA, Pippen AM, Cherwek H, Taylor DA, Annex BH. Alterations in endothelial cell proliferation and apoptosis contribute to vascular remodeling following hind-limb ischemia in rabbits. Vasc Med 2002;7:87-91.

[24] Dash BC, Rethore G, Monaghan M, Fitzgerald K, Gallagher W, Pandit A. The influence of size and charge of chitosan/polyglutamic acid hollow spheres on cellular internalization, viability and blood compatibility. Biomaterials 2010;31:8188-97.

[25] Champion JA, Walker A, Mitragotri S. Role of particle size in phagocytosis of polymeric microspheres. Pharm Res 2008;25:1815-21.

[26] Zhu Y, Tramper J. Novel applications for microbial transglutaminase beyond food processing. Trends Biotechnol 2008;26:559-65.

[27] Dinerman JL, Mehta JL, Saldeen TG, Emerson S, Wallin R, Davda R, et al. Increased neutrophil elastase release in unstable angina pectoris and acute myocardial infarction. J Am Coll Cardiol 1990;15:1559-63.

[28] Silvestre JS, Mallat Z, Duriez M, Tamarat R, Bureau MF, Scherman D, et al. Antiangiogenic effect of interleukin-10 in ischemia-induced angiogenesis in mice hindlimb. Circ Res 2000;87:448-52.

[29] Brito LA, Chandrasekhar S, Little SR, Amiji MM. Non-viral eNOS gene delivery and transfection with stents for the treatment of restenosis. Biomed Eng Online 2010;9:56.

[30] Montes de Oca M, Torres SH, De Sanctis J, Mata A, Hernandez N, Talamo C. Skeletal muscle inflammation and nitric oxide in patients with COPD. Eur Respir J 2005;26:390-7.

[31] Holladay C, Power K, Sefton M, O'Brien T, Gallagher WM, Pandit A. Functionalized scaffold-mediated interleukin 10 gene delivery significantly improves survival rates of stem cells in vivo. Mol Ther 2011;19:969-78.

[32] O'Connor DM, O'Brien T. Nitric oxide synthase gene therapy: progress and prospects. Expert Opin Biol Ther 2009;9:867-78.

[33] Ren JG, Jie C, Talbot C. How PEDF prevents angiogenesis: a hypothesized pathway. Med Hypotheses 2005;64:74-8.

[34] Battegay EJ, Rupp J, Iruela-Arispe L, Sage EH, Pech M. PDGF-BB modulates endothelial proliferation and angiogenesis in vitro via PDGF beta-receptors. Journal Cell Biol 1994;125:917-28.

[35] Hellberg C, Ostman A, Heldin CH. PDGF and vessel maturation. Recent Results Cancer Res 2010;180:103-14.

[36] van Hal PT, Hopstaken-Broos JP, Prins A, Favaloro EJ, Huijbens RJ, Hilvering C, et al. Potential indirect anti-inflammatory effects of IL-4. Stimulation of human monocytes, macrophages, and endothelial cells by IL-4 increases aminopeptidase-N activity (CD13; EC 3.4.11.2). J Immunol 1994;153:2718-28.

[37] Woodward EA, Kolesnik TB, Nicholson SE, Prele CM, Hart PH. The anti-inflammatory actions of IL-4 in human monocytes are not mediated by IL-10, RP105 or the kinase activity of RIPK2. Cytokine 2012;58:415-23.

[38] Mentlein R, Held-Feindt J. Angiogenesis factors in gliomas: a new key to tumour therapy? Die Naturwissenschaften 2003;90:385-94.

[39] Nyberg P, Xie L, Kalluri R. Endogenous inhibitors of angiogenesis. Cancer Res 2005;65:3967-79.

[40] Ribatti D. Endogenous inhibitors of angiogenesis: a historical review. Leuk Res 2009;33:638-44.

[41] Bellingham CM, Woodhouse KA, Robson P, Rothstein SJ, Keeley FW. Self-aggregation characteristics of recombinantly expressed human elastin polypeptides. Biochim Biophys Acta 2001;1550:6-19.

[42] Rethore G, Mathew A, Naik H, Pandit A. Preparation of chitosan/polyglutamic acid spheres based on the use of polystyrene template as a nonviral gene carrier. Tissue Eng Part C Methods 2009;15:605-13.

[43] Rethore G, Pandit A. Use of templates to fabricate nanoscale spherical structures for defined architectural control. Small 2010;6:488-98.

[44] Bubnis WA, Ofner CM, 3rd. The determination of epsilon-amino groups in soluble and poorly soluble proteinaceous materials by a spectrophotometric method using trinitrobenzenesulfonic acid. Anal Biochem 1992;207:129-33.

[45] Peng X, Wang J, Lassance-Soares RM, Najafi AH, Sood S, Aghili N, et al. Gender differences affect blood flow recovery in a mouse model of hindlimb ischemia. Am J Physiol Heart Circ Physiol 2011;300:H2027-34.

[46] Shireman PK, Quinones MP. Differential necrosis despite similar perfusion in mouse strains after ischemia. J Surg Res 2005;129:242-50.

[47] Garcia Y, Breen A, Burugapalli K, Dockery P, Pandit A. Stereological methods to assess tissue response for tissue-engineered scaffolds. Biomaterials 2007;28:175-86.

Figure 1

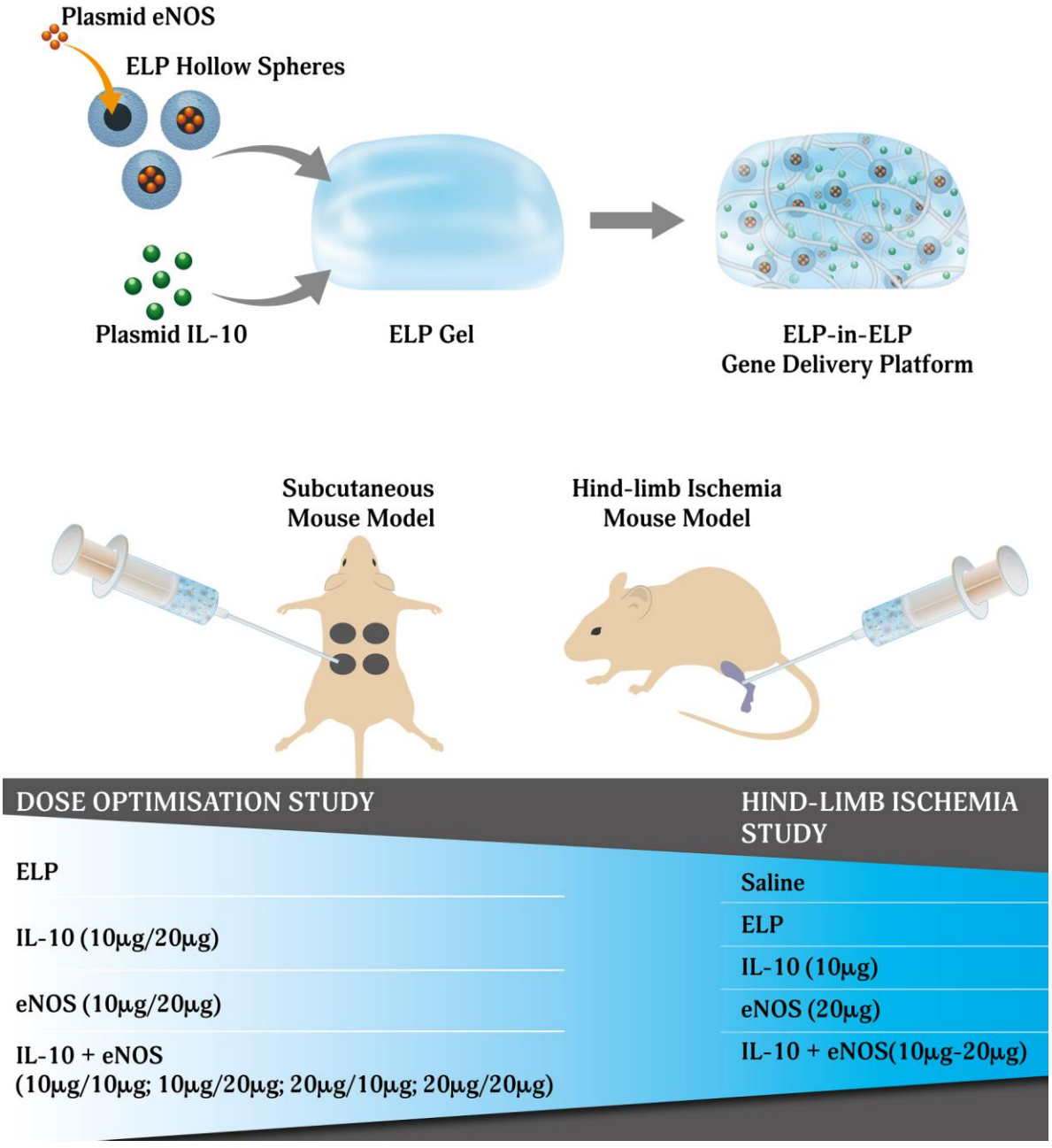
Plasmid eNOS
ELP Hollow Spheres
Plasmid IL-10
ELP Gel
ELP-in-ELP
Gene Delivery Platform
Subcutaneous
Mouse Model
Hind-limb Ischemia
Mouse Model
DOSE OPTIMISATION STUDY
ELP
IL-10 (10μg/20μg)
eNOS (10μg/20μg)
IL-10 + eNOS
(10μg/10μg; 10μg/20μg; 20μg/10μg; 20μg/20μg)
HIND-LIMB ISCHEMIA STUDY
Saline
ELP
IL-10 (10μg)
eNOS (20μg)
IL-10 + eNOS(10μg-20μg)

Figure 2

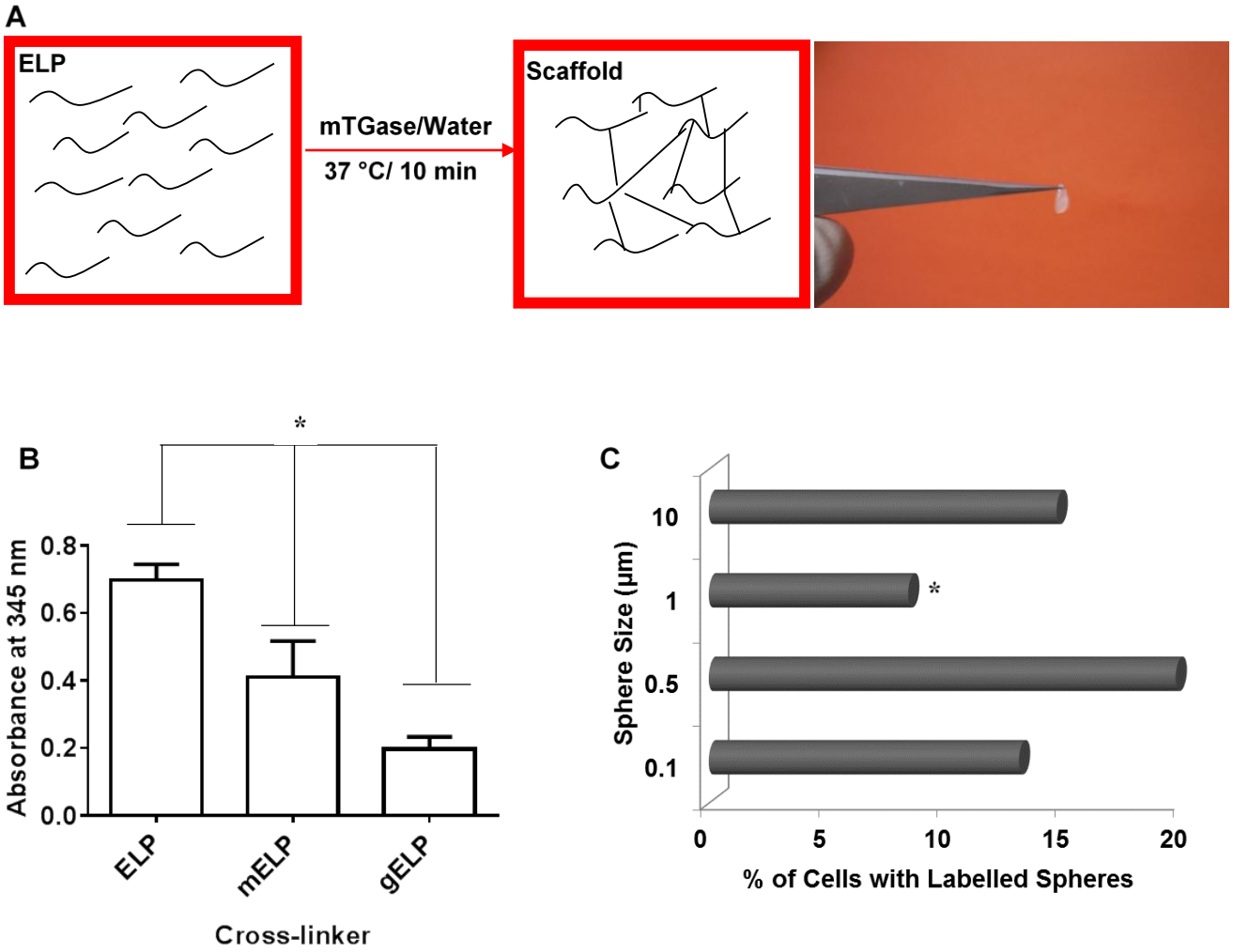
A
ELP
mTGase/Water
37 °C/ 10 min
Scaffold
B
Absorbance at 345 nm
0.0
0.2
0.4
0.6
0.8
*
ELP
mELP
gELP
Cross-linker
C
Sphere Size (µm)
10
1
0.5
0.1
*
0
5
10
15
20
% of Cells with Labelled Spheres
D
% Cumulative Release of pDNA
0
10
20
30
40
50
60
70
80
90
100
Scaffold + Polyplex
Sphere + Polyplex
*
*
*
*
1
4
7
10
Days

Figure 3

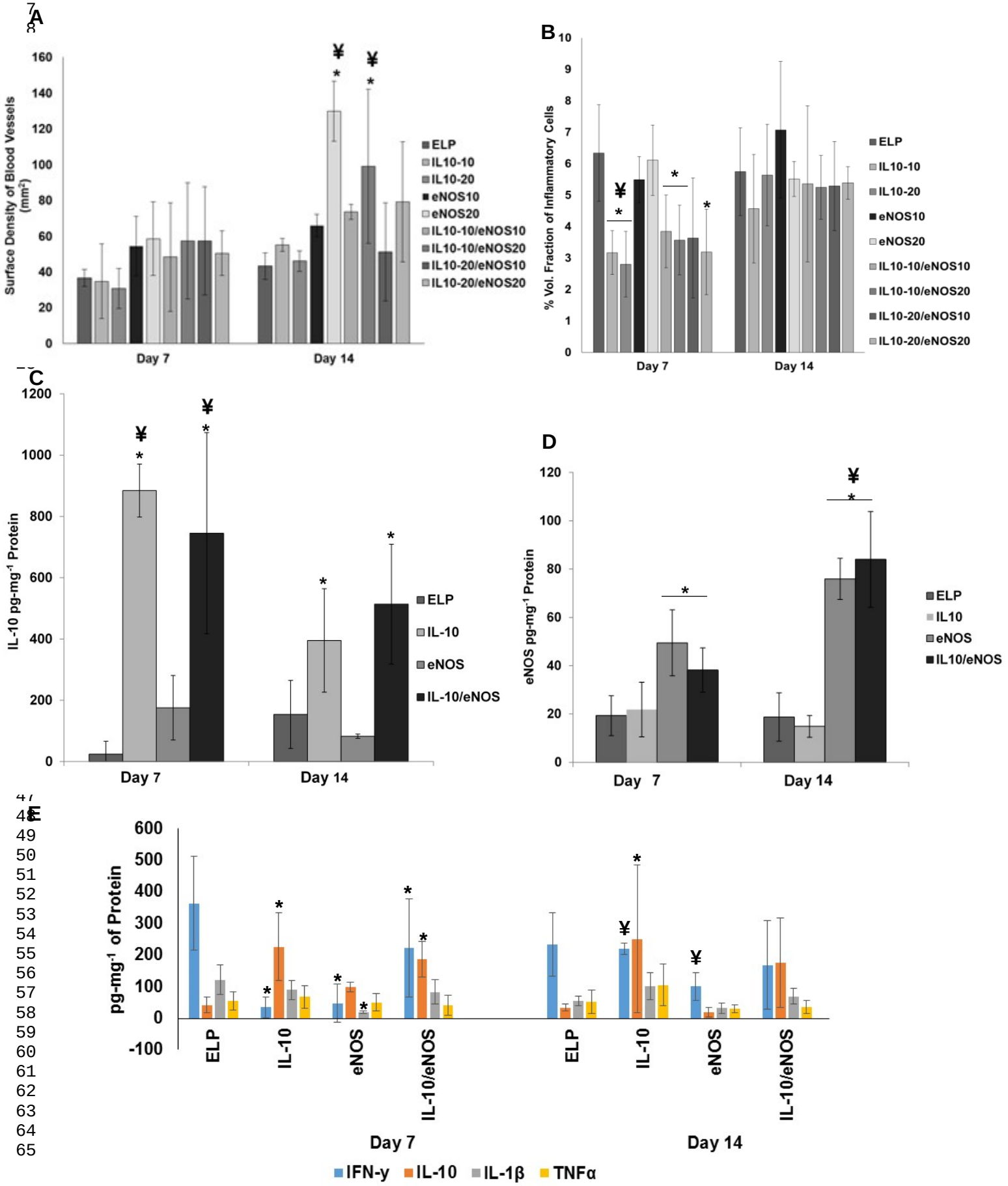
A
Surface Density of Blood Vessels (mm²)
Day 7
Day 14
ELP
IL10-10
IL10-20
eNOS10
eNOS20
IL10-10/eNOS10
IL10-10/eNOS20
IL10-20/eNOS10
IL10-20/eNOS20
B
% Vol. Fraction of Inflammatory Cells
C
IL-10 pg-mg-1 Protein
IL-10
eNOS
IL-10/eNOS
D
eNOS pg-mg-1 Protein
IL10
IL10/eNOS
E
pg-mg-1 of Protein
IFN-γ
IL-1β
TNFα

Figure 4

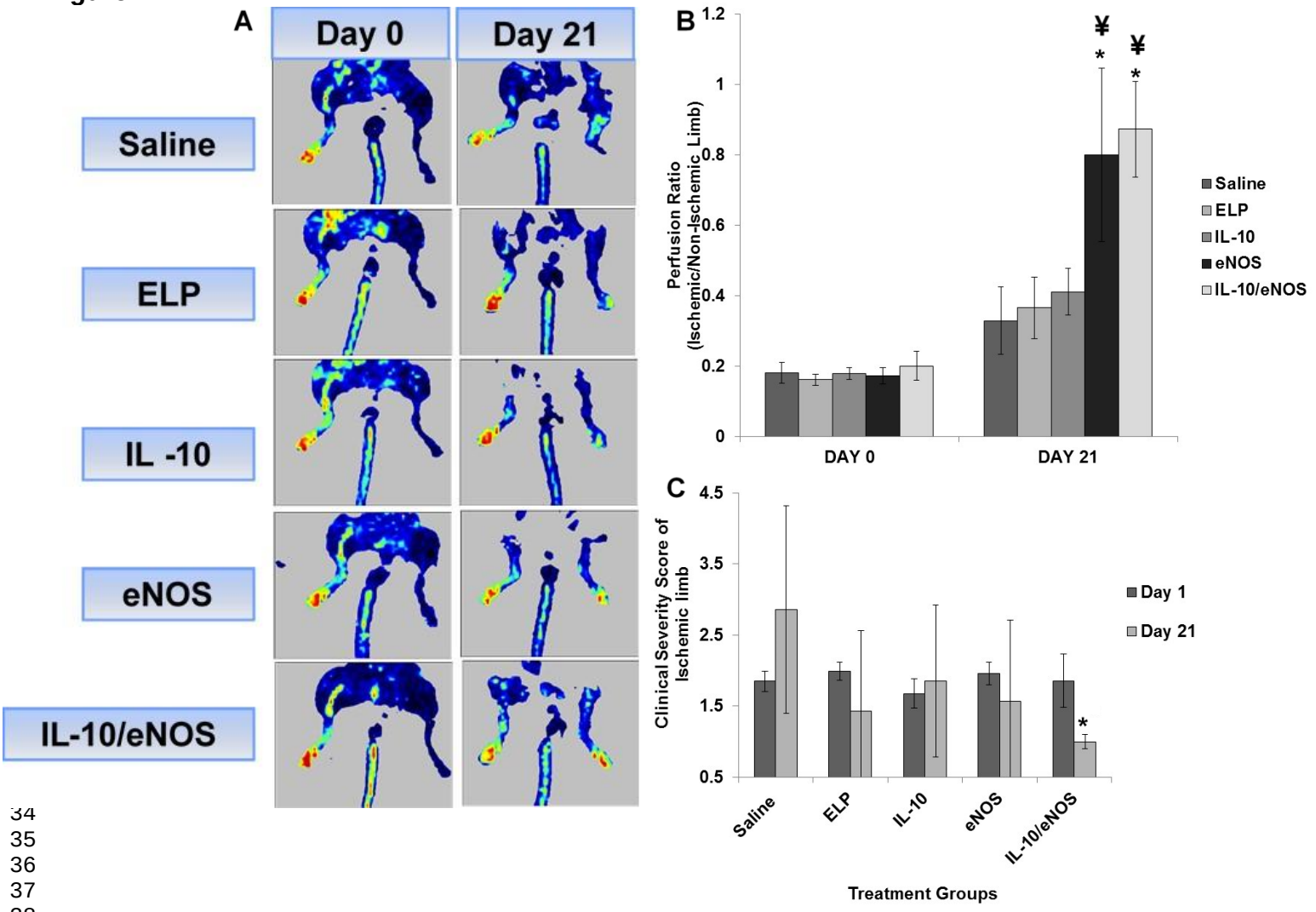
A
Day 0
Day 21
Saline
ELP
IL -10
eNOS
IL-10/eNOS
B
Perfusion Ratio (Ischemic/Non-Ischemic Limb)
DAY 0
DAY 21
Saline
ELP
IL-10
eNOS
IL-10/eNOS
C
Clinical Severity Score of Ischemic limb
Day 1
Day 21
Saline
ELP
IL-10
eNOS
IL-10/eNOS
Treatment Groups
D
IL-10 pg-mg-1 Protein
Day 7
Day 21
ELP
IL-10
eNOS
IL-10/eNOS
E
eNOS pg-mg -1 Protein
Day 7
Day 21
ELP
IL10
eNOS
IL10/eNOS

Figure 5

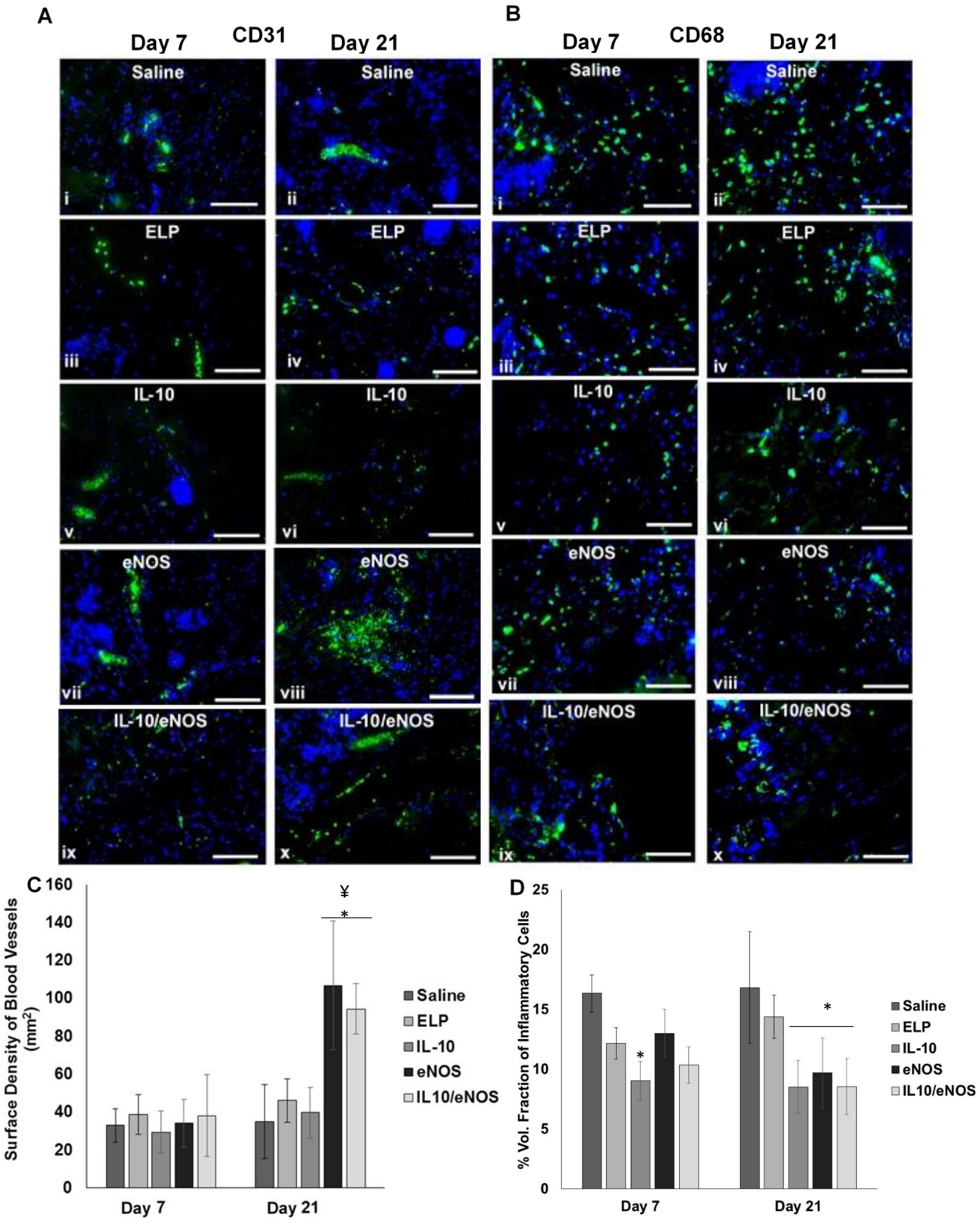
A
Day 7
CD31
Day 21
Saline
ELP
IL-10
eNOS
IL-10/eNOS
i
ii
iii
iv
v
vi
vii
viii
ix
x
B
Day 7
CD68
Day 21
C
Surface Density of Blood Vessels (mm²)
160
140
120
100
80
60
40
20
0
¥
*
Day 7
Day 21
Saline
ELP
IL-10
eNOS
IL10/eNOS
D
% Vol. Fraction of Inflammatory Cells
25
20
15
10
5
0
*
*
Day 7
Day 21
Saline
ELP
IL-10
eNOS
IL10/eNOS

Figure 6

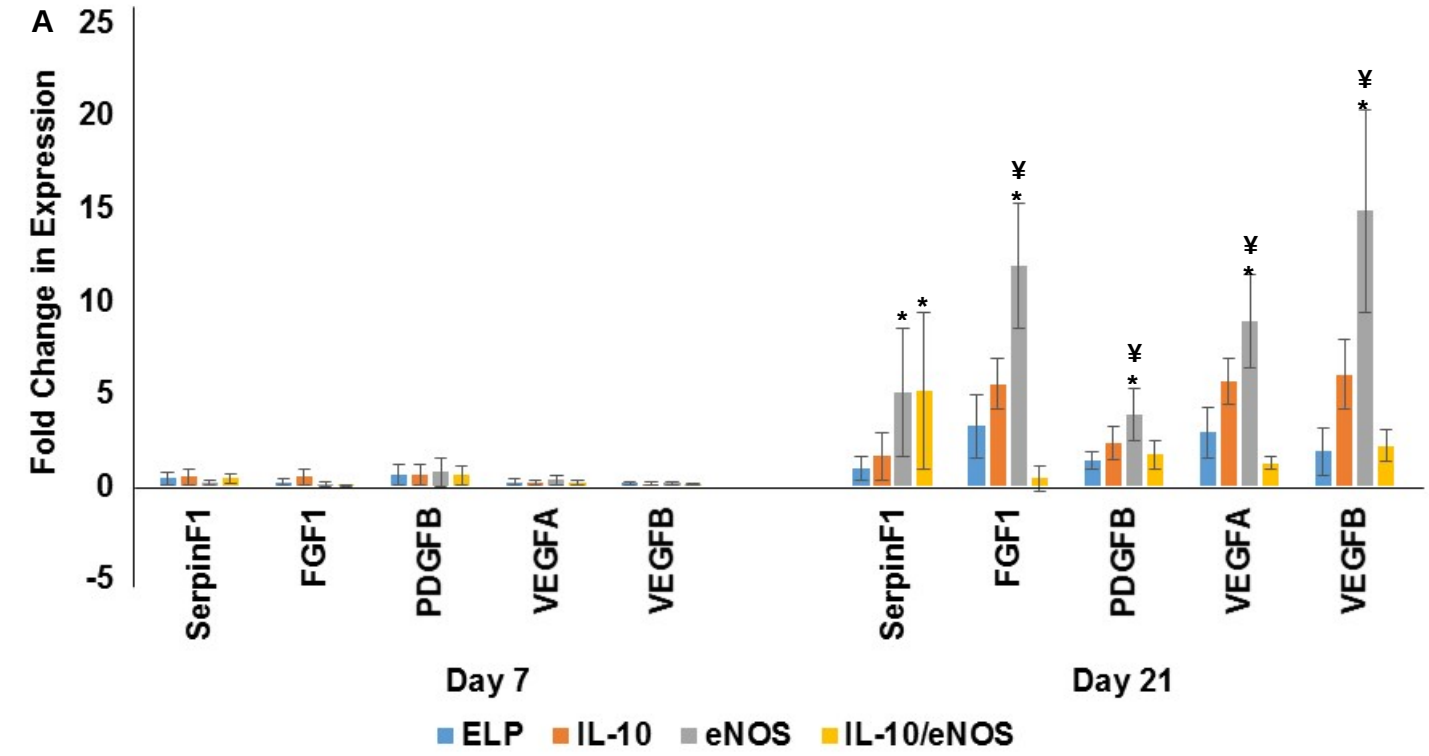
A
Fold Change in Expression
25
20
15
10
5
0
-5
SerpinF1
FGF1
PDGFB
VEGFA
VEGFB
SerpinF1
FGF1
PDGFB
VEGFA
VEGFB
Day 7
Day 21
ELP
IL-10
eNOS
IL-10/eNOS

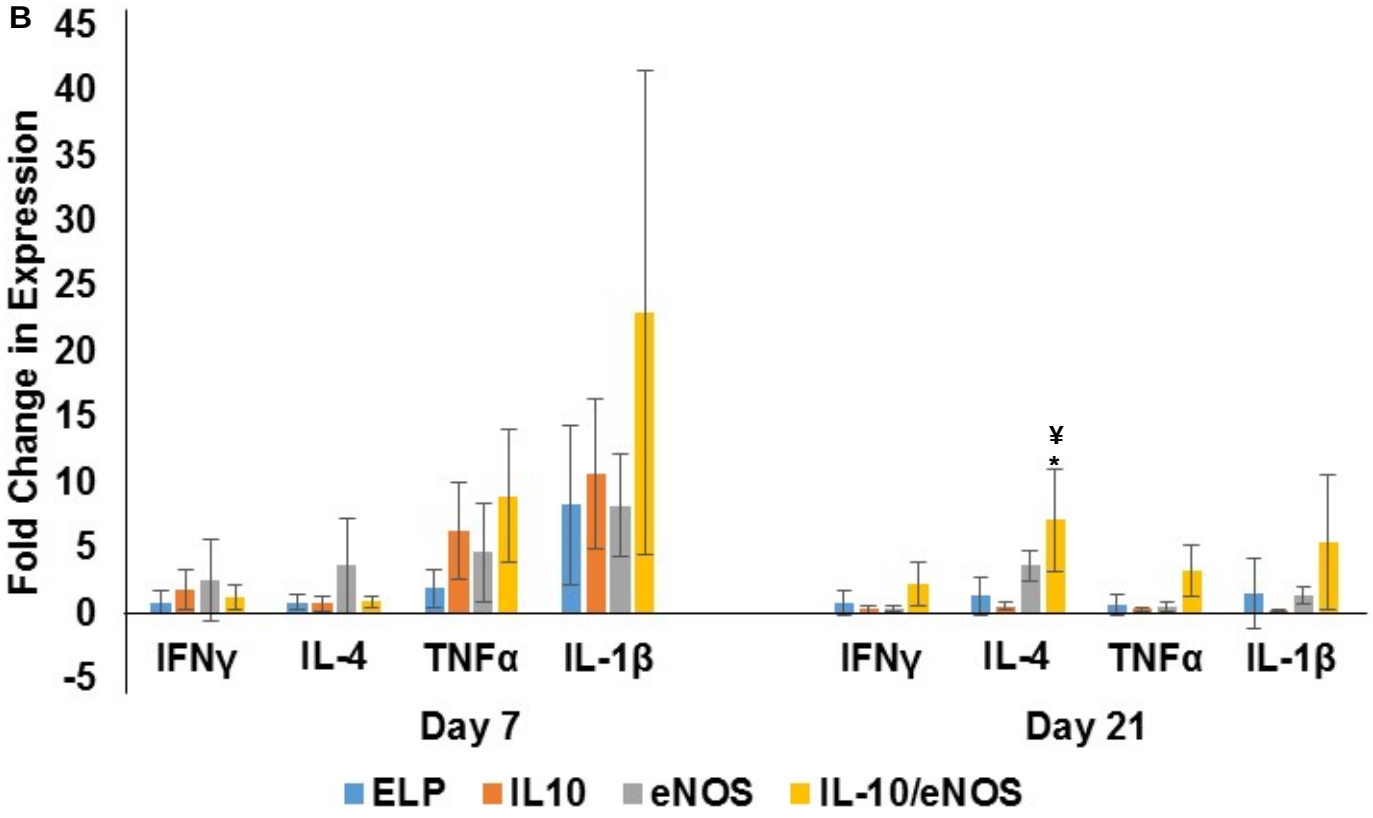
B
Fold Change in Expression
45
40
35
30
25
20
15
10
5
0
-5
IFNγ
IL-4
TNFα
IL-1β
IFNγ
IL-4
TNFα
IL-1β
Day 7
Day 21
ELP
IL10
eNOS
IL-10/eNOS

Figure 7

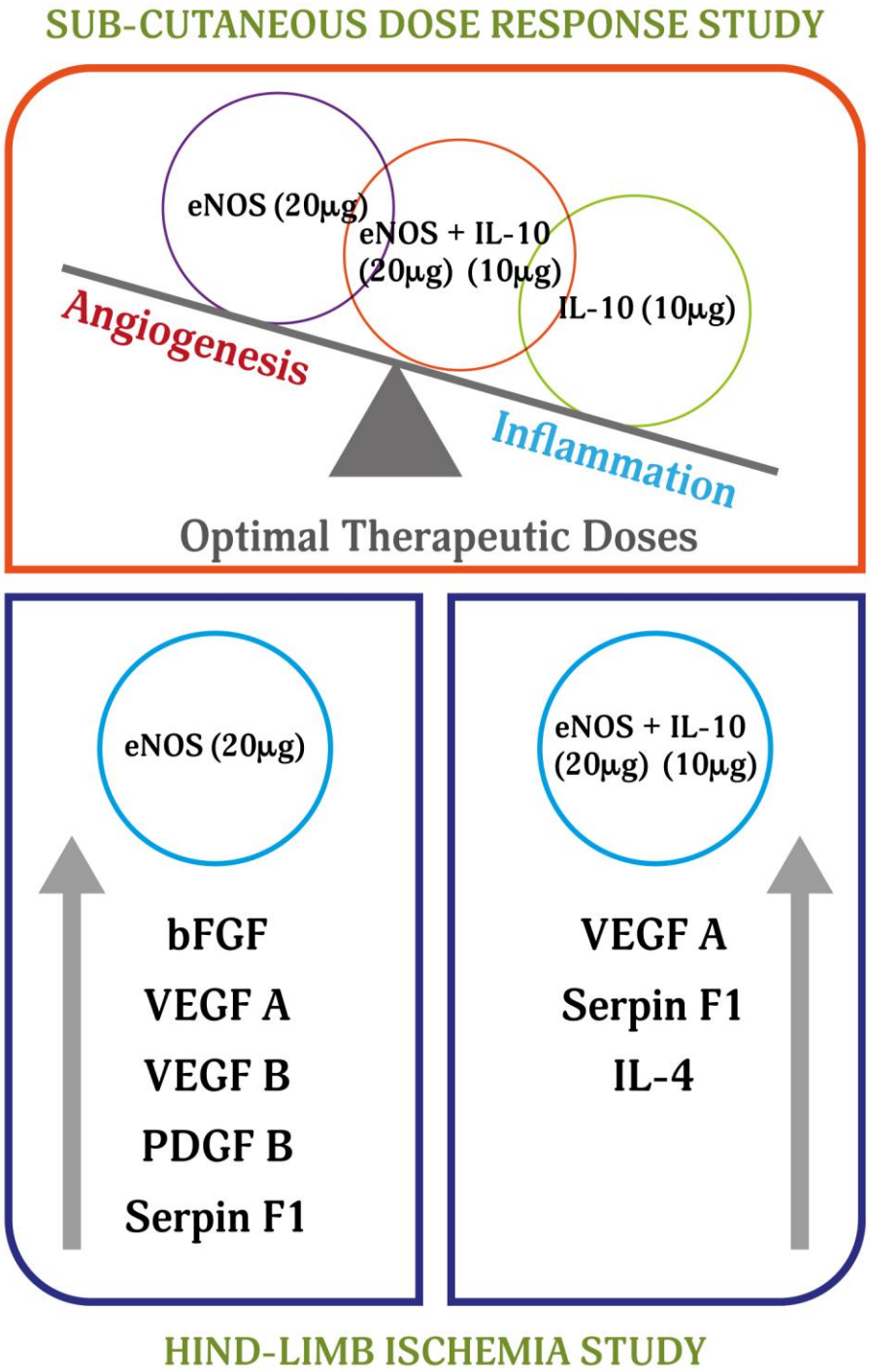
SUB-CUTANEOUS DOSE RESPONSE STUDY
eNOS (20μg)
eNOS + IL-10
(20μg) (10μg)
IL-10 (10μg)
Angiogenesis
Inflammation
Optimal Therapeutic Doses
eNOS (20μg)
bFGF
VEGF A
VEGF B
PDGF B
Serpin F1
eNOS + IL-10
(20μg) (10μg)
VEGF A
Serpin F1
IL-4
HIND-LIMB ISCHEMIA STUDY

Figure Legends

Figure 1: A schematic showing the overall goal of this study. The study includes an *in vitro* fabrication of the ELP-in-ELP injectable system and delivery of the therapeutic genes heNOS and hIL-10 in a subcutaneous study to determine a therapeutic dose for heNOS and hIL-10 and a final *in vivo* study in a mouse model of HLI.

Figure 2: (A) A schematic representation of the injectable elastin-like polypeptide scaffold fabrication method. Elastin-like polypeptide and microbial transglutaminase (mTGase) mixture solution in water forms the scaffold when incubated at 37 °C. Photographic image showing solidified elastin-like polypeptide based scaffold after gelation. (B) TNBSA analysis to characterize the cross-linking of elastin-like polypeptide scaffold with mTGase enzyme of 100U/g of ELP. Glutaraldehyde and elastin-like polypeptide alone were used as positive and negative control respectively. (C) Flow cytometry data, elucidating the effect of size on the internalization efficiency of elastin-like polypeptide hollow spheres into human umbilical vein endothelial cells respectively at 24 h incubation. (D) Cumulative release profile of pDNA/polyplex from the injectable system: elastin-like polypeptide scaffold/polyplex and elastin-like polypeptide hollow spheres/polyplex at 37 ºC and treated with elastase. All the data are represented as the mean ± standard deviation (n = 3, p < 0.05). Statistical significance by one-way ANOVA. * represents statistical significant difference.

Figure 3: (A) and (B) Surface density of blood vessels and volume fraction of inflammatory cells respectively in the subcutaneous implant area, days 7 and 14. (C) and (D) Human IL-10 and eNOS expression level respectively in the subcutaneous implant for days 7 and 14. (E) Screening of inflammatory cytokines expressed in the subcutaneous implant by days 7 and 14. Elastin-like polypeptide scaffold only was kept as a control for all these experiments. Statistical

significance by one-way ANOVA (n = 6, p < 0.05). * represents statistical significance between tretament groups of one time point and ¥ represents statistical significance between day 7 and 14 time points.

Figure 4: (A) Improvement of blood flow recovery at the ischemic site following eNOS treatment. Representative Laser Doppler perfusion imaging (LDPI) at week 0 (10 min after the ischemic surgery) and week 3 is shown. In these digital color-coded images, maximum perfusion values are in red, medium values in yellow to green, and lowest values in dark blue. (B) Blood perfusion measurement of ischemic limb in mouse model. (C) Assessment of clinical severity of the ischemic limb. Measurements were performed by observing parameters such as 1) plantar flexion but mild discoloration, 2) no plantar flexion and mild discoloration, 3) no plantar flexion and moderate to severe discoloration and 4) necrosis. (D) and (E) Human IL-10 and eNOS expression level respectively in the ischemic tissue, days 7 and 21. Statistical significance by one-way ANOVA (n = 7, p < 0.05). * represents statistical significance between treatment groups of one time point; ¥ represents statistical significance between day 7 and 21 time points.

Figure 5: (A) and (B) CD31 and CD 68 staining of blood vessels respectively (stained as green cells) at days 7 and 21 in various treatments in the ischemic study. (i, ii) Saline; (iii, iv) ELP; (v, vi) IL-10; (vii, viii) eNOS; (ix, x) IL-10/eNOS. The scale bar represents 100 μm. (C) and (D) Surface density of blood vessels and volume fraction of inflammatory cells respectively in the ischemic tissue for days 7 and 21. Statistical significance by one-way ANOVA (n = 7, p < 0.05). * represents statistical significance between tretament groups of one time point and ¥ represents statistical significance between day 7 and 21 time points.

Figure 6: RT-PCR data showing differential regulation of (A) angiogenic and (B) inflammatory factors with respect to treatment groups ELP, IL-10, eNOS and IL-10/eNOS in the ischemic tissue on days 7 and 21. Statistical significance was determined by one way ANOVA ($n = 3$, $p < 0.05$). * represents a significant difference in the upregulation of a factor on day 21 compared to its early time point day 7. ¥ represents a significant difference in the upregulation of a factor on day 21 compared to the rest of the treatment groups.

Figure 7: The schematic summarizes dose response study to determine therapeutic doses of eNOS and IL-10 to enhance angiogenesis and modulate inflammation and the therapeutic goal (in terms of changes in the angiogenesis and inflammation level in the ischemic tissue) achieved by the treatment group eNOS and IL-10/eNOS and the key factors associated with these changes at a molecular level.

Table 1: Nine treatment groups used for the subcutaneous dose study.

Treatment groups	**Abbreviation**	**hIL-10 *p*DNA (µg)**	**heNOS *p*DNA (µg)**
Scaffold/Hollow sphere	ELP		
Scaffold-IL 10/Hollow sphere	IL10-10	10	
Scaffold-IL 10/Hollow sphere	IL10-20	20	
Scaffold/Hollow sphere-eNOS	eNOS10		10
Scaffold/Hollow sphere-eNOS	eNOS20		20
Scaffold-IL10/Hollow sphere-eNOS	IL10-10/eNOS10	10	10
Scaffold-IL10/Hollow sphere-eNOS	IL10-10/eNOS20	10	20
Scaffold-IL10/Hollow sphere-eNOS	IL10-20/eNOS10	20	10
Scaffold-IL10/Hollow sphere-eNOS	IL10-20/eNOS20	20	20

Supplementary Files

Click here to download Supplementary Files: Supplementary Information-Biomaterials.docx